



Intraoperative and biomechanical studies of human vastus lateralis and vastus medialis sarcomere length operating range



Jongsang Son^a, Andy Indresano^b, Kristin Sheppard^b, Samuel R. Ward^{b,c}, Richard L. Lieber^{a,b,d,*}

^a Shirley Ryan AbilityLab (formerly Rehabilitation Institute of Chicago), IL, United States

^b Department of Orthopaedic Surgery, University of California San Diego, La Jolla, CA, United States

^c Department of Radiology, University of California San Diego, La Jolla, CA, United States

^d Research Service, Hines V.A. Hospital, Maywood, IL, United States

ARTICLE INFO

Article history:

Accepted 26 November 2017

Keywords:

Muscle physiology
Sarcomere length
Biomechanical modeling
Patellar pain

ABSTRACT

The vast majority of musculoskeletal models are not validated against primary experimental data. Conversely, most human experimental measurements are not explained theoretically using models to provide a mechanistic understanding of experimental results. Here we present a study with both primary human data and primary modeling data. Intraoperative sarcomere length was measured on the human vastus lateralis (VL) and vastus medialis (VM) muscles ($n = 8$) by laser diffraction. These data were compared to a biomechanical model based on muscle architecture and moment arms obtained independently from cadaveric specimens ($n = 9$). Measured VL sarcomere length ranged from about $3.2 \mu\text{m}$ with the knee flexed to 45° to $3.8 \mu\text{m}$ with the knee flexed to 90° . These values were remarkably close to theoretical predictions. Measured VM sarcomere length ranged from $3.6 \mu\text{m}$ with the knee flexed to 45° to $4.1 \mu\text{m}$ with the knee flexed to 90° . These values were dramatically longer than theoretical predictions. Our measured sarcomere length values suggest that human vasti may have differing functions with regard to knee extension and patellar stabilization. This report underscores the importance of validating experimental data to theoretical models and vice versa.

Published by Elsevier Ltd.

1. Introduction

Elucidating the design and function of human skeletal muscles is required to understand normal function, pathological conditions and suggest surgical interventions to recover function after injury (Fridén and Lieber, 2002; Gans, 1982; Lieber and Fridén, 2000; Lieber and Ward, 2011). Across the human body, it could be argued that quadriceps muscles are the most important functional muscle group. Their function is obviously critical for locomotion and opposing gravity (Perry, 1992). However, their strength is also related to clinical problems such as patellar pain and tracking and locomotion efficiency and there is even evidence that quadriceps strength loss can predict the onset of osteoarthritis (Mahir et al., 2016). At the tissue level, human vastus lateralis muscle biopsies represent the gold standard for study of human muscle (Bergstrom, 1975; Lexell et al., 1986; Sjöström et al., 1982; Willan et al., 2002) so it is not an understatement to state that

what is known about human muscle fiber types and plasticity is primarily known about the vastus lateralis muscle.

A detailed understanding of the design and function of human muscles is hampered by the lack of tools available to provide the types of detailed studies in humans that have often been performed in animal models. One of the most important parameters needed to understand the design and function of muscle is sarcomere length (Lieber and Fridén, 2000; Lieber and Ward, 2011). The muscle sarcomere is the functional unit of force generation in skeletal muscle and its length is an excellent predictor of active muscle force (Edman, 1966; Gordon et al., 1966; Winters et al., 2011). Our laboratory has published sarcomere length values in humans for over twenty years (Lieber et al., 1994) and sarcomere lengths in animal models for over thirty years (Lieber and Baskin, 1983; Lieber et al., 1983), primarily using laser diffraction approaches (Lieber et al., 1984). Laser diffraction provides a robust sarcomere length value because it spatially averages across hundreds of thousands of sarcomeres (see Table 1 of reference Young et al., 2014) to yield a single value with a resolution of 5–10 nm. In cadaveric samples, sarcomere length measurements across the muscle can provide sarcomere length estimates for the entire muscle (Takahashi et al., 2007) while, in patients, sarcomere length is

* Corresponding author at: Shirley Ryan AbilityLab, 355 E. Erie Street, Chicago, IL 60611, United States.

E-mail address: rlieber@ric.org (R.L. Lieber).

typically measured only in single muscle region exposed based on surgical indications (Lieber et al., 1994; Ward et al., 2009).

In light of the fact that laser diffraction studies are limited to surgical patients, it is encouraging that microendoscopy has been recently emerged for intravital use in human volunteers not undergoing surgery (Llewellyn et al., 2008). Because microendoscopy is much less invasive than laser diffraction, sarcomere lengths can now be recorded from muscles not previously available. This represents a significant technical advance in the field, perhaps even enabling dynamic sarcomere length measurements.

Another approach used to understand musculoskeletal function, is to create biomechanical models based on previously measured muscle, joint and tendon properties. The vast majority of these theoretical models are not validated against primary experimental data (Hicks et al., 2015). It is also fair to critique most human experimental measurements as not being explained theoretically using models to provide a mechanistic understanding of experimental results. Our goal was to measure human quadriceps sarcomere length during knee flexion in joint replacement patients and then to validate these measurements against a model generated from independent measurements obtained from cadaveric specimens. Because sarcomere lengths from one of these same muscles was recently reported (Chen et al., 2016), it is also possible to compare laser diffraction and microendoscopy methods for the vastus lateralis muscle.

With regard to the modeling approach, biomechanical and anatomical data are often combined to make predictions. Because a high degree of inter-individual variation occurs, it is not clear whether it is justified to combine disparate datasets collected on different individuals and combining them to create models. Addressing this question is relevant to the current trend toward developing patient-specific models. Thus, the purpose of this study was to compare the sarcomere length range of the human vasti between directly measured values and those obtained via biomechanical modeling.

2. Methods

2.1. Intraoperative sarcomere length

Sarcomere length was measured from human patients ($n = 7$) using a protocol approved by the Committee on the Use of Human Subjects at the University of California, San Diego and the Department of Veterans Affairs, San Diego. Measurements were performed on vastus lateralis (VL) and vastus medialis (VM) muscles of patients undergoing total knee replacement. After exposing the VL and VM, a specially designed muscle clamp was used to obtain a muscle sample when the knee was flexed to 45° (measured from 0° as full extension) and with the knee flexed to 90° . This method was previously validated against intraoperative laser diffraction in rabbit muscle (Ward et al., 2009). During surgery, a small segment of each muscle was atraumatically isolated by blunt dissection. Samples were obtained from adjacent fascicles on the distal pole of both muscles.

After the muscle sample was clamped, the section of muscle within the jaws of the clamp was resected and immediately placed in Formalin to fix the biopsy specimen in its *in vivo* configuration. After 2-days of fixation, muscle bundles were dissected and placed on glass slides and sarcomere length was measured by laser diffraction (see below).

2.2. Moment arm measurement

To provide the biomechanical input data for a theoretical model, cadaveric lower extremities were used for determination

of moment arm and quadriceps muscle architecture ($n = 9$). In addition to the VL and VM, rectus femoris (RF) and vastus intermedius (VI) were dissected from extremities with care taken to maintain the integrity of the skin and associated tissues of the knee. Muscles were removed and their architectural properties determined using methods previously described (see below).

The dissected knee was mounted onto a mechanical jig securing the distal femur by Steinman pins to vertical braces while an additional pin engaged the middle third of the tibia allowing knee flexion and extension (Fig. 1). Thirty-gauge stainless steel sutures were secured to the distal stumps of quadriceps tendon and routed to electrogoniometers recreating the line of force for each muscle. These stainless steel sutures were secured to toothed nylon cables and connected to nonbacklash gears mounted to potentiometers as described by An et al. (1983) and placed under 500 g tension. Neutral (0°) was defined as alignment of the tibia and the distal femur in the sagittal plane. The knee was passed manually from 0 to 100° of flexion. Individual excursions of quadriceps tendons and joint angular displacements were digitized simultaneously. Each excursion trial was repeated three times.

Tendon excursion was differentiated with respect to joint angle yielding moment arm as a function of joint angle. Before differentiating, excursion data were resampled every 10° to avoid superfluous noise. Moment arm-knee angle relationships were then fit by stepwise polynomial regression using an algorithm developed to minimize the influence of the fitting method on the resulting equation (Burkholder and Lieber, 1996; Loren et al., 1996). This was done by including only the polynomial terms that significantly improved the curve fit (p -to-enter = 0.05) and not requiring all lower order terms to be included beneath the highest order term. The explanation power of the stepwise polynomial regression was confirmed according to the different maximum polynomial order ranging 0–10. As a result, 3rd-order stepwise regression was used for further analysis because 3rd-order stepwise fitting explained 90% of the variability in the raw data (Fig. 3A).

2.3. Muscle architecture

For architectural measurements, fascicles were dissected from specimens that were Formalin-fixed with the body fully supine. Thus, the hip and knee were at approximately 0° and the ankles at approximately 30° of plantarflexion. Three regions of each muscle loosely defined as proximal, middle and distal, were measured

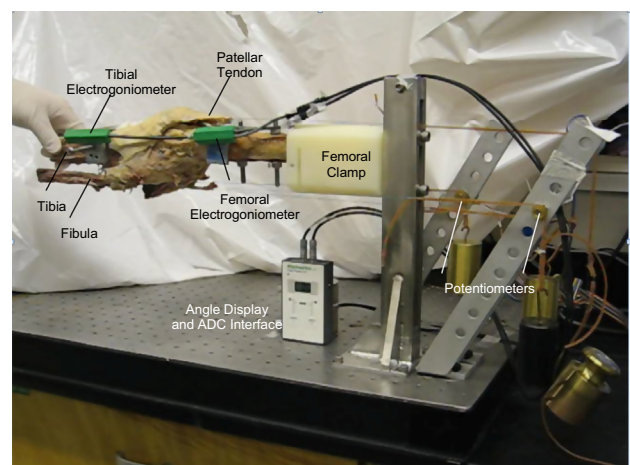


Fig. 1. Experimental apparatus to measure knee extension moment arm. Cadaveric specimens were mounted on a specially designed jig and patellar tendon excursion measured indirectly via potentiometers. Joint angle was measured directly via electrogoniometers mounted to the distal femur and proximal tibia.

according to the methods developed by Sacks and Roy (1982) applied by Ward et al. (2009) to fixed human lower extremity muscles. Briefly, muscle specimens were removed from buffer, gently blotted dry, and mass determined (m). Muscle length (L^M) was defined as the distance from the origin of the most proximal fibers to insertion of the most distal fibers. Raw fiber length (L^{Fr}) was measured from the previously mapped three regions in each muscle using a digital caliper (accuracy, 0.01 mm). Surface pennation angle (α) was measured in each of these regions with a standard goniometer. Fascicles then were placed in mild sulfuric acid solution (15% v/v) for 30 mins to partially digest surrounding connective tissue and then rinsed in phosphate-buffered saline. Three small muscle fiber bundles (consisting of approximately 20 single cells) were then isolated from each muscle region and mounted on slides. Bundle sarcomere length (L^S) was determined by laser diffraction as described by Lieber et al. (1984). To allow comparisons of fiber length among muscles (Felder et al., 2005; Lieber, 1997), optimal fiber length (L_o^F) was calculated as $L_o^F = L^{Fr}(L_o^S/L^S)$, where L_o^S is the optimal sarcomere length for human muscle (i.e., 2.7 μm , based on quantitative electron microscopy as described in reference Lieber et al., 1994). Pennation angle at optimal fiber length, α_o , was estimated with an assumption of constant muscle thickness as $\alpha_o = \sin^{-1}(\sin \alpha (L^{Fr}/L_o^F))$. Physiologic cross-sectional area (PCSA) was calculated as $PCSA = mL_o^F \cos \alpha / \rho$, where ρ is muscle density (i.e., 1.056 g/cm^3) (Ward and Lieber, 2005), which was used to determine maximum isometric force by multiplying the PCSA by a specific tension of 61 N/cm^2 . The optimal fiber length, pennation angle at optimal fiber length, and maximum isometric force were used as parameters for a musculotendon model in the following section. All muscle architecture properties are shown in Table 1.

2.4. Quadriceps musculoskeletal model

A modified Hill-type musculotendon model (Thelen, 2003) was used to calculate sarcomere length with respect to knee angle, with a slight modification (see Appendix). A constant activation was set to 0.01 (i.e., 1% of maximum isometric contraction) for resting state the conditions under which the muscle architecture data were obtained. The active fiber force-length relationship is represented as a Gaussian function including one parameter (i.e., a shape factor, γ). The value of γ was set to 0.15 in this study to approximate the force-length relationship of sarcomeres in human lower limb muscles (Cutts, 1988). The passive fiber force-length relationship was represented by an exponential function including two parameters (i.e., an exponential shape factor, k^{PE} , and passive muscle strain

due to maximum isometric contraction, ϵ_0^M). The values of k^{PE} and ϵ_0^M were set to 4 and 0.6, respectively. Total fiber force was determined as summation of active and passive fiber forces. Among five parameters, only the tendon strain due to maximum isometric contraction, ϵ_0^T , was modified to 0.08 (i.e., 8%) based on *in vivo* ultrasound measurements obtained during maximum isometric contraction of human VL (Stafilidis et al., 2005), and it was assumed that the value of ϵ_0^T for each muscle was the same. The value for other four parameters not mentioned here was set to the same value as in reference (Thelen, 2003). Using the model, tendon slack length was first determined by finding the value at which the fiber length measured in the cadaver matched the value predicted by the model at a given muscle activation of 1% and musculotendon length measured in the cadaver. Once tendon slack length was defined, fiber and tendon lengths were then determined by iteratively adjusting the lengths until the absolute difference between normalized forces developed by fiber and tendon at the lengths was less than the program tolerance (i.e., 1×10^{-3}) at a given muscle activation and each of musculotendon length corresponding to knee angles of 0° to 110° . Sarcomere length with respect to knee angle was then determined as $L^S(\theta) = L_o^S(L^F(\theta)/L_o^F)$ where L^S is modeled sarcomere length, and L^F modeled fiber length.

2.5. Statistical analysis

To compare the intraoperative sarcomere lengths between VM and VL, a paired *t*-test was performed with a significance level (α) of 0.05, using SPSS Statistics (version 21, IBM, Chicago).

3. Results

3.1. Intraoperative sarcomere length

Sarcomere length measured in VM was significantly longer than that measured in VL (Fig. 2A; $p < .05$). Sarcomere length increased by $\sim 0.5 \mu\text{m}$ for both muscles when the knee was flexed from 45° to 90° (Fig. 2A). This was true whether the data were used from paired comparisons where VL and VM were measured from one and the same subject (Fig. 2A, $n = 4$ paired subjects) or whether a global data set was used, created by combining the paired data with three other isolated measurements of VM muscles (Fig. 2B). Importantly, at both angles of 45° and 90° of knee flexion, VM sarcomere length was significantly greater than VL sarcomere length, by almost $0.5 \mu\text{m}$. These data demonstrate that sarcomere length is consistent measured among humans for a given muscle and that sarcomere length for VM is consistently longer than that of the VL.

Table 1
Muscle architectural properties.

	Vastus lateralis	Vastus medialis
Muscle mass (g) ^a	353.02 \pm 125.83	230.18 \pm 88.47
Musculotendon length (cm) ^a	44.65 \pm 3.05	41.64 \pm 3.29
Fiber length (cm) ^a	7.80 \pm 1.26	7.77 \pm 0.98
Sarcomere length (μm) ^a	2.27 \pm 0.12	2.22 \pm 0.22
Pennation angle ($^\circ$) ^a	21.11 \pm 7.91	31.30 \pm 6.11
PCSA (cm^2) ^b	34.0 \pm 14.3	20.0 \pm 8.7
Optimal fiber length (cm) ^b	9.33 \pm 1.80	9.59 \pm 1.73
Pennation angle at optimal fiber length ($^\circ$) ^b	17.44 \pm 6.11	25.60 \pm 7.28
Maximum isometric force (N) ^b	2072.6 \pm 875.2	1222.3 \pm 530.2
Tendon slack length (cm) ^c	37.22 \pm 3.00	34.80 \pm 3.43

^a Measured value from cadaver.

^b Calculated value based on measurements (please see Muscle architecture in Method).

^c Calculated value at which the fiber length measured in the cadaver matched the value predicted by the model at a given muscle activation of 1% and musculotendon length measured in the cadaver (please see Quadriceps musculoskeletal model in Method).

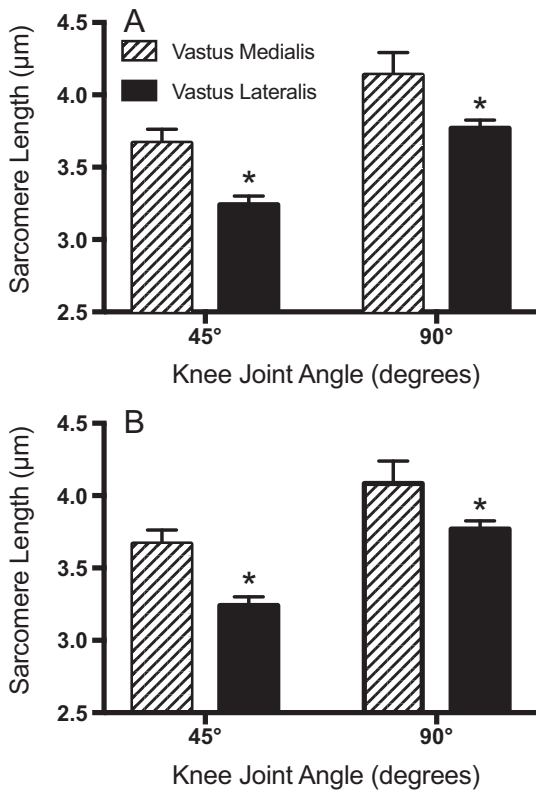


Fig. 2. Vastus lateralis (filled bars) and vastus medialis (hatched bars) sarcomere length measured by laser diffraction with the knee in 45° and 90° of flexion. (A) Experimental data from paired subjects ($n = 4$ data points from each muscle). (B) Experimental data from paired subjects combined with additional independent VM measurements ($n = 4$ data points from VL and $n = 7$ data points from VM).

3.2. Knee extension moment arm

Moment arms calculated by differentiating the excursion-joint angle data revealed the expected nonlinear relationship between moment arm and knee flexion angle (red line, Fig. 3B). As previously noted (An et al., 1983), nonlinear moment arms can be difficult to calculate by differentiation of excursion-joint angle data since higher polynomials fit data better than lower orders, but the differential of the excursion-moment arm data yields moment arm curves that are very different. We thus used an objective criterion to select polynomial order based on the fit with a coefficient of determination greater than 0.9 which was achieved using a third order polynomial (Fig. 3A). Knee extension moment arm recreated the moment arm profile previously reported by others (Buford et al., 1997; Grood et al., 1984; Herzog and Read, 1993; Spoor et al., 1990) and was approximately the arithmetic average of the literature in magnitude (Fig. 3B). Additionally, the average moment arm value faithfully represented the raw data obtained from each of the ten specimens (Fig. 3C) which gives us confidence that our analytical approach did not induce the actual shape or magnitude of the moment arm relationship.

3.3. Sarcomere length operating range

Predicted and measured sarcomere length revealed close agreement for the VL (red line and symbols in Fig. 4A) and worse agreement for VM (Fig. 4B). For VL, as the knee was flexed from full extension (0°) to full flexion (110°) sarcomere length was predicted to increase from 2.3 to 3.8 µm (Fig. 4A) corresponding to sarcomere lengths on the ascending, plateau and descending limbs of the

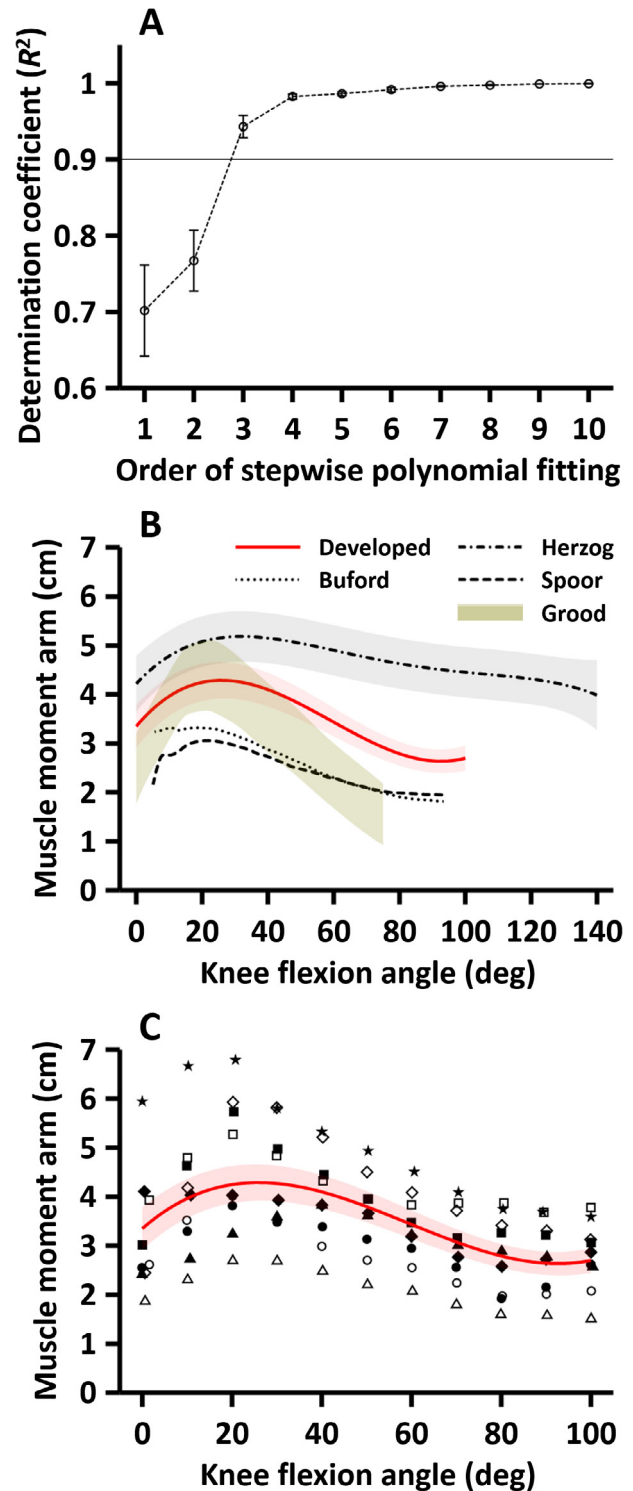


Fig. 3. Calculation of moment arm from cadaveric specimens. (A) Coefficient of determination (R^2) from data set as a function of order used to fit data. The third order fit was the lowest order fit that explained 90% of experimental data variation and was thus used to describe the moment arm results. (B) Knee extension moment arm as a function of knee joint angle based on cadaveric data ($n = 9$). Data shown are mean \pm 1SEM compared to four other studies. (C) Average knee extension moment arm data superimposed upon raw data from the current study.

human length tension curve (Gordon et al., 1966). Sarcomere lengths predicted from the model were within a standard error of those measured intra-operatively (Fig. 4A). These data provide strong support for the experimental approach used here (use of

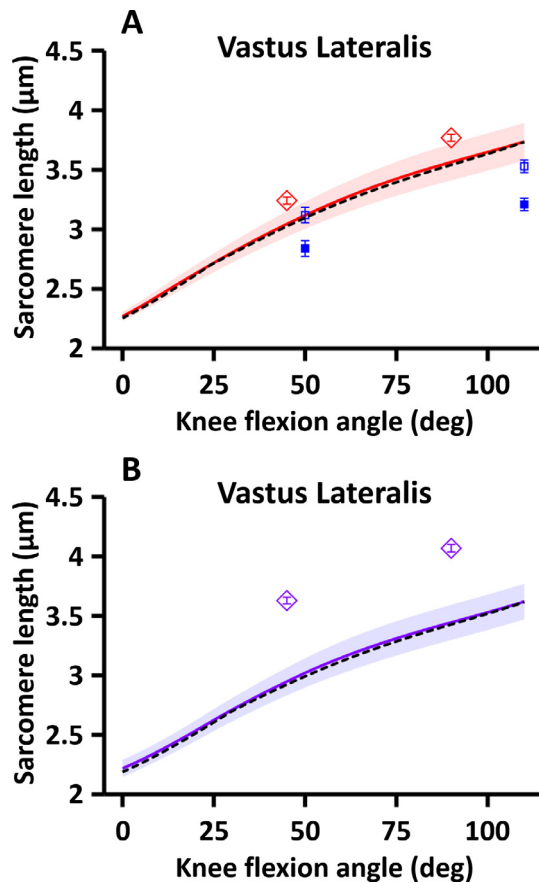


Fig. 4. Comparison between subject-specific predicted sarcomere length-joint angle relationship (solid line with shaded area representing ± 1 SEM) to experimental data. (A) Comparison for the vastus lateralis. Note that experimental data (red squares) are within the experimental error of model predictions. Also shown are previously published data for the VL from [Chen et al. \(2016\)](#) for data reported in their study (filled blue squares) and their data divided by 0.91 to “uncorrected” for tissue distortion. See discussion for details of this comparison. (B) Comparison for the vastus medialis. Note that experimental data (purple diamonds) are over 3 SEM from the model predictions. Potential reasons for the discrepancy between model and experimental data are provided in the Discussion. Dashed line represents sarcomere length modeled by combined averaged muscle and joint data.

cadaveric data, subject specific cadaveric muscle architecture and subject specific cadaveric moment arms) as well as the intraoperative measuring technique. For comparison, the recently published data from [Chen et al. \(2016\)](#) are also presented in blue ([Fig. 4A](#)). According to their methods, measured data were multiplied by 0.91 to account for fiber deformation around the probe tip. These data are presented as solid squares ([Fig. 4A](#)). However, sarcomere length measurements are subject to numerous artifacts (see discussion below) and thus, since we have not “corrected” our data, we provide the data reported by [Chen et al. \(2016\)](#) divided by 0.91 to compare their original data to ours ([Fig. 4A](#), open blue squares). Overall, our prediction for vastus lateralis sarcomere length, the raw data from [Chen et al.](#), and the raw data from our intraoperative values are all remarkably close. These data thus support the notion that VL sarcomere length operating range is known and traverses the sarcomere length-tension fairly uniformly. Peak VL force is predicted to occur at $\sim 20^\circ$ of flexion.

Unfortunately, results for the VM were more disparate when comparing measured to predicted sarcomere lengths and there are no comparable data available from microendoscopy. Predicted sarcomere length ranged from $\sim 2.2 \mu\text{m}$ with the knee fully extended to ~ 3.7 with the knee flexed to 110° . This suggests that peak VM force would occur with the knee at near full extension.

With regard to sarcomere length predictions, measured sarcomere length at 45° was ~ 3.6 (compared to a model prediction of $\sim 3 \mu\text{m}$) and $\sim 4.1 \mu\text{m}$ at 90° of flexion (compared to a model prediction of $\sim 3.5 \mu\text{m}$). Thus, our measured values were ~ 4 standard errors away from model predictions. This discrepancy is discussed below. For both the VM and VL, the two modeling approaches (patient-specific vs. lumped parameters) yielded essentially the same results (compare solid and dashed lines in [Fig. 4](#)). As an index of agreement between modeling approaches, the root mean squared error (RMSE) was calculated between the two predictions. For the VL, RMSE value was $0.011 \mu\text{m}$ and for the VM it was $0.018 \mu\text{m}$, both extremely low ([Fig. 4](#)).

4. Discussion

The purpose of this paper was to predict and measure sarcomere length operating range independently in the human VL and VM muscles. The results of this study indicate that, in spite of using exactly the same methodological approaches for the two muscles, predictions for VL are much closer than the predictions for VM. In addition, the intraoperative data reveal that the sarcomere length operating range of the VM is biased toward longer sarcomere lengths compared to the VL. These data provide valuable insights into quadriceps muscle function, arguably one of the most important muscle groups in the human body. They also provide insight into experimental approaches to musculoskeletal model validation.

4.1. Challenges to measuring sarcomere length

Our laboratory has been measuring sarcomere length in humans for over twenty years ([Lieber et al., 1994](#)) and in skeletal muscle for over thirty years ([Lieber and Baskin, 1983](#)). Since sarcomere length has a profound impact on force generation in muscle, it is one of the most important parameters required to understand a particular muscle’s function but is rarely directly measured. It is extremely difficult to measure sarcomere length in living humans. One reason it is difficult is for the obvious reason of exposing the tissue. Recent advances in intravital microendoscopy ([Llewellyn et al., 2008](#)) now allow sarcomere length measurement from muscles that were previously only available by surgical exposure. Unfortunately, microendoscopy uses second harmonic generation to slowly image only about a dozen sarcomeres, which is a very small sample in the landscape of muscle fibers and fascicles (see Table 1 of reference [Young et al., 2014](#)). Additionally, due to the relatively large size of the tip (1 mm) compared to the diameter of the muscle fibers ($50 \mu\text{m}$) the probe subjects the muscle fibers to distortion. Because sarcomere length varies by about 10% throughout human muscles ([Lieber et al., 1990](#); [Lieber et al., 1992](#); [Ward et al., 2009](#); [Ward et al., 2006](#); [Wickiewicz et al., 1983](#)), it is not clear whether this amount of sampling is representative of the entire muscle. Indeed, the standard deviations of the values reported by microendoscopy exceed those reported by laser diffraction ([Chen et al., 1993](#)). Laser diffraction suffers from a different limitation—it can only be used in skeletal muscles that are surgically exposed, necessarily limiting its use to patient populations. In addition, because the laser device has to be placed beneath the fiber bundles, the technique requires great care so that sarcomeres are not over-stretched since muscle tissue is fairly compliant. In prior studies, distortion due to slight elevation of the biopsy increased sarcomere length by about $0.1 \mu\text{m}$ ([Lieber et al., 1994](#)). Indeed, it is exceedingly difficult to try to “calibrate” living muscle sarcomere lengths obtained by diffraction against fixed tissue values. We reported this twenty years ago when measuring intraoperative sarcomere length of the extensor carpi

radialis brevis (ECRB) muscle (see Fig. 2 of reference Lieber et al., 1994). While there was general agreement among these values, it was surprising to us that biopsy sarcomere lengths were actually more variable than those obtained *in vivo*. This suggests that the fixation process itself does not necessarily retain sarcomeres in their *in vivo* configuration. This is why we back calculated the results from Chen et al. (2016) for comparison to our intraoperative data (Fig. 4A) since the 0.91 “correction factor” they obtained from rat skeletal muscle may or may not be appropriate. We believe that their uncorrected data in Fig. 4A (open blue squares) are most comparable to our intraoperative laser diffraction data. In the future, we anticipate more generalizable results in humans using resonant reflection spectroscopy (Young et al., 2014) combined with optical fiber differential interferometry (Young et al., 2017) via fiber optics.

4.2. Comparison of musculoskeletal models to experimental data

This study validated sarcomere length predicted from architectural and kinematic data in cadaveric subjects against direct intraoperative measurements. These data reinforce the idea that independent validation of experimental studies provide a mechanistic underpinning for results obtained is critical (Hicks et al., 2015). For the VL, the results are quite appealing—predicted sarcomere length from the experimental model are extremely close to measured values either by laser diffraction or intravital microendoscopy (Fig. 4A). The VL appears to generate peak force at about 20° of flexion, where maximum force production is required (Perry, 1992). For the VM, measured sarcomere lengths are systematically longer than the VL at the same joint angle. The reason for this bias is not clear but it may be that the higher force generated by VM with the knee nearly fully extended is required to stabilize the patella against the lateral force produced by the VL during locomotion. The reason for the lack agreement between VM experiment and theory is also not explained clearly—measured values considerably exceed model prediction, by many standard errors. In this case, the model prediction is not near the experimentally measured values even though precisely the same experimental approach was used as that VL. The reason for this disagreement is not clear but we posit the following three possibilities: (1) The VM data are obtained from patients about to undergo total knee replacement with limited range of motion. It is possible that this resulted in an adaptation of the muscle to more extended knee joint angles and decrease in serial sarcomere number resulting in longer sarcomere lengths. (2) It is also possible that VM data do not agree with model predictions because intraoperative values were taken from the distal pole of the VM, the VMO. The VMO has been implicated as being important in patellar stabilization and it has been suggested, based on electromyographic data, that preferential VMO activation may play a role in patellar pain syndrome (Souza and Gross, 1991). (3) It is possible, as stated by others (Blemker and Delp, 2006), that the use of a single moment arm for the entire muscle is simply not realistic. If this is true, then the values for the VMO by itself would require a smaller moment arm compared to the value for the rest of the muscle. It should be noted that upon checking the average sarcomere lengths along the vastus medialis muscle reported previously (Ward et al., 2009), no systematic variations from proximal to distal were obtained.

4.3. Comparison of modeling approaches

Sarcomere length operating range modeled above can be calculated using two general approaches. (1) summarizing architectural data, separately summarizing kinematic data and then combining the two data sets to calculate sarcomere length operating range or, (2) modeling sarcomere length operating range of each speci-

men using that subject’s specific muscle and joint data and then averaging the resulting sarcomere length–joint angle curves to yield the average result. The first approach simulates the general approach used in the literature and the second approach simulates the “subject-specific” modeling approach that assumes that muscle and joint properties within an individual are complementary. In this study, both approaches yielded the same result supporting the general approach used by the biomechanical modeling community.

In summary, the current experiments demonstrate that the sarcomere length operating range of the VL appears to straddle the entire length–tension curve whereas the sarcomere length operating range of the VM is biased toward longer values. These ranges may have significant functional implications. The fact that experimental and theoretical data fit very well for the VL but not for the VM underscore the need for increased resolution of musculoskeletal modeling and the need for validation studies in this field.

Acknowledgements

This work was supported by the National Institutes of Health grant R24HD050837 and the Department of Veterans Affairs. The authors declare no conflict of interest with regard to this work.

Appendix A. Supplementary materials

Supplementary data associated with this article can be found, in the online version, at <https://doi.org/10.1016/j.jbiomech.2017.11.038>.

References

- An, K.N., Ueba, Y., Chao, E.Y., Cooney, W.P., Linscheid, R.L., 1983. Tendon excursion and moment arm of index finger muscles. *J. Biomech.* 16, 419–425.
- Bergstrom, J., 1975. Percutaneous needle biopsy of skeletal muscle in physiological and clinical research. *Scand. J. Clin. Lab. Invest.* 35, 609–616.
- Blemker, S.S., Delp, S.L., 2006. Rectus femoris and vastus intermedius fiber excursions predicted by three-dimensional muscle models. *J. Biomech.* 39, 1382–1391.
- Buford Jr., W.L., Ivey Jr., F.M., Malone, J.D., Patterson, R.M., Peare, G.L., Nguyen, D.K., Stewart, A.A., 1997. Muscle balance at the knee—moment arms for the normal knee and the ACL-minus knee. *IEEE Trans. Rehabil. Eng.* 5, 367–379.
- Burkholder, T.J., Lieber, R.L., 1996. Stepwise regression is an alternative to splines for fitting noisy data. *J. Biomech.* 29, 235–238.
- Chen, M.-J.C., Shih, C.-L., Wang, K., 1993. Nebulin as an actin zipper: A two-module nebulin fragment promotes actin nucleation and stabilizes actin filaments. *J. Biol. Chem.* 268, 20327–20334.
- Chen, X., Sanchez, G.N., Schinitzer, M.J., Delp, S.L., 2016. Changes in sarcomere lengths of the human vastus lateralis muscle with knee flexion measured using *in vivo* microendoscopy. *J. Biomech.* 49, 2989–2994.
- Cutts, A., 1988. The range of sarcomere lengths in the muscles of the human lower limb. *J. Anat.* 160, 79.
- Edman, K., 1966. The relation between sarcomere length and active tension in isolated semitendinosus fibres of the frog. *J. Physiol. (Lond)* 183, 407–417.
- Felder, A., Ward, S.R., Lieber, R.L., 2005. Sarcomere length measurement permits high resolution normalization of muscle fiber length in architectural studies. *J. Exp. Biol.* 208, 3275–3279.
- Fridén, J., Lieber, R.L., 2002. Mechanical considerations in the design of surgical reconstructive procedures. *J. Biomech.* 35, 1039–1045.
- Gans, C., 1982. Fiber architecture and muscle function. In: *Exercise and Sport Science Reviews*. Franklin University Press, Lexington, MA, pp. 160–207.
- Gordon, A.M., Huxley, A.F., Julian, F.J., 1966. The variation in isometric tension with sarcomere length in vertebrate muscle fibres. *J. Physiol. (Lond.)* 184, 170–192.
- Grood, E.S., Suntay, W.J., Noyes, F.R., Butler, D.L., 1984. Biomechanics of the knee-extension exercise. Effect of cutting the anterior cruciate ligament. *J. Bone Joint Surg. Am.* 66, 725–734.
- Herzog, W., Read, L.J., 1993. Lines of action and moment arms of the major force-carrying structures crossing the human knee joint. *J. Anat.* 182 (Pt 2), 213–230.
- Hicks, J.L., Uchida, T.K., Seth, A., Rajagopal, A., Delp, S.L., 2015. Is my model good enough? Best practices for verification and validation of musculoskeletal models and simulations of movement. *J. Biomech. Eng.* 137, 020905.
- Lexell, J., Downham, D., Sjöström, M., 1986. Distribution of different fibre types in human skeletal muscles. Fibre type arrangement in m. vastus lateralis from three groups of healthy men between 15 and 83 years. *J. Neurol. Sci.* 72, 211–222.

- Lieber, R.L., 1997. Muscle fiber length and moment arm coordination during dorsi- and plantarflexion in the mouse hindlimb. *Acta Anat. (Basel)* 159, 84–89.
- Lieber, R.L., Baskin, R.J., 1983. Intersarcomere dynamics of single muscle fibers during fixed-end tetani. *J. Gen. Physiol.* 82, 347–364.
- Lieber, R.L., Fazeli, B.M., Botte, M.J., 1990. Architecture of selected wrist flexor and extensor muscles. *J. Hand. Surg. [Am.]* 15A, 244–250.
- Lieber, R.L., Friden, J., 2000. Functional and clinical significance of skeletal muscle architecture. *Muscle Nerve* 23, 1647–1666.
- Lieber, R.L., Jacobson, M.D., Fazeli, B.M., Abrams, R.A., Botte, M.J., 1992. Architecture of selected muscles of the arm and forearm: anatomy and implications for tendon transfer. *J. Hand. Surg. [Am.]* 17A, 787–798.
- Lieber, R.L., Loren, G.J., Friden, J., 1994. In vivo measurement of human wrist extensor muscle sarcomere length changes. *J. Neurophysiol.* 71, 874–881.
- Lieber, R.L., Roos, K.P., Lubell, B.A., Cline, J.W., Baskin, R.J., 1983. High speed digital data acquisition of sarcomere length from isolated skeletal and cardiac muscle cells. *IEEE Trans. Biomed. Eng.* 30, 50–57.
- Lieber, R.L., Ward, S.R., 2011. Skeletal muscle design to meet functional demands. *Philos. Trans. R. Soc. Lond. B. Biol. Sci.* 366, 1466–1476.
- Lieber, R.L., Yeh, Y., Baskin, R.J., 1984. Sarcomere length determination using laser diffraction. Effect of beam and fiber diameter. *Biophys. J.* 45, 1007–1016.
- Llewellyn, M.E., Barretto, R.P., Delp, S.L., Schnitzer, M.J., 2008. Minimally invasive high-speed imaging of sarcomere contractile dynamics in mice and humans. *Nature* 454, 784–788.
- Loren, G.J., Shoemaker, S.D., Burkholder, T.J., Jacobson, M.D., Fridén, J., Lieber, R.L., 1996. Human wrist motors: Biomechanical design and application to tendon transfers. *J. Biomech.* 29, 331–342.
- Mahir, L., Belhaj, K., Zahi, S., Lmidmani, F., El Fatimi, A., 2016. Importance of isokinetic in knee osteoarthritis. *Ann. Phys. Rehabil. Med.* 59S, e155–e156.
- Perry, J., 1992. *Gait Analysis: Normal and Pathological Function*. Slack Inc., Thorofare, NJ.
- Sacks, R.D., Roy, R.R., 1982. Architecture of the hind limb muscles of cats: Functional significance. *J. Morphol.* 173, 185–195.
- Sjöström, M., Kidman, S., Henriksson-Larsen, K., Ångquist, K.A., 1982. Z- and M-band appearance in different histochemically defined types of human skeletal muscle fibers. *J. Histochem. Cytochem.* 30, 1–11.
- Souza, D.R., Gross, M.T., 1991. Comparison of vastus medialis obliquus: vastus lateralis muscle integrated electromyographic ratios between healthy subjects and patients with patellofemoral pain. *Phys. Ther.* 71, 310–316.
- Spoor, C.W., van Leeuwen, J.L., Meskers, C.G., Titulaer, A.F., Huson, A., 1990. Estimation of instantaneous moment arms of lower-leg muscles. *J. Biomech.* 23, 1247–1259.
- Stafilidis, S., Karamanidis, K., Morey-Klapsing, G., DeMonte, G., Brüggemann, G.-P., Arampatzis, A., 2005. Strain and elongation of the vastus lateralis aponeurosis and tendon in vivo during maximal isometric contraction. *Eur. J. Appl. Physiol.* 94, 317–322.
- Takahashi, M., Ward, S., Lieber, R.L., 2007. Intraoperative single-site sarcomere length measurement accurately reflects whole muscle sarcomere length. *J. Hand. Surg. [Am.]* 32, 612–617.
- Thelen, D.G., 2003. Adjustment of muscle mechanics model parameters to simulate dynamic contractions in older adults. *J. Biomech. Eng.* 125, 70–77.
- Ward, S.R., Eng, C.M., Smallwood, L.H., Lieber, R.L., 2009. Are Current Measurements of Lower Extremity Muscle Architecture Accurate? *Clin. Orthop. Relat. Res.* 467, 1074–1082.
- Ward, S.R., Hentzen, E.R., Smallwood, L.H., Eastlack, R.K., Burns, K.A., Fithian, D.C., Friden, J., Lieber, R.L., 2006. Rotator cuff muscle architecture: implications for glenohumeral stability. *Clin Orthop Rel Res* 448, 157–163.
- Ward, S.R., Kim, C.W., Eng, C.M., Gottschalk, L.J.t., Tomiya, A., Garfin, S.R., Lieber, R.L., 2009. Architectural analysis and intraoperative measurements demonstrate the unique design of the multifidus muscle for lumbar spine stability. *J. Bone Joint Surg. Am.* 91, 176–185.
- Ward, S.R., Lieber, R.L., 2005. Density and hydration of fresh and fixed skeletal muscle. *J. Biomech.* 38, 2317–2320.
- Ward, S.R., Takahashi, M., Winters, T.M., Kwan, A., Lieber, R.L., 2009. A novel muscle biopsy clamp yields accurate in vivo sarcomere length values. *J. Biomech.* 42, 193–196.
- Wickiewicz, T.L., Roy, R.R., Powell, P.L., Edgerton, V.R., 1983. Muscle architecture of the human lower limb. *Clin. Orthop. Rel. Res.* 179, 275–283.
- Willan, P.L., Ransome, J.A., Mahon, M., 2002. Variability in human quadriceps muscles: quantitative study and review of clinical literature. *Clin. Anat.* 15, 116–128.
- Winters, T.M., Takahashi, M., Lieber, R.L., Ward, S.R., 2011. Whole muscle length-tension relationships are accurately modeled as scaled sarcomeres in rabbit hindlimb muscles. *J. Biomech.* 44, 109–115.
- Young, K.W., Dayanidhi, S., Lieber, R.L., 2014. Polarization gating enables sarcomere length measurements by laser diffraction in fibrotic muscle. *J. Biomed. Opt.* 19, 117009.
- Young, K.W., Kuo, B.P., O'Connor, S.M., Radic, S., Lieber, R.L., 2017. In vivo sarcomere length measurement in whole muscles during passive stretch and twitch contractions. *Biophys. J.* 112, 805–812.
- Young, K.W., Radic, S., Myslivets, E., O'Connor, S.M., Lieber, R.L., 2014. Resonant reflection spectroscopy of biomolecular arrays in muscle. *Biophys. J.* 107, 2352–2360.